Published in final edited form as:
J Phys Chem A. 2010 September 9; 114(35): 9507–9514. doi:10.1021/jp102272z.

Development and validation of a ReaxFF reactive force field for Cu-cation/water interactions and copper metal/metal oxide/metal hydroxide condensed phases

Adri C.T. van Duin[a,*], **Vyacheslav S. Bryantsev**[b], **Mamadou S. Diallo**[b], **William A. Goddard III**[b], **Obaidur Rahaman**[c], **Douglas J. Doren**[c], **David Raymand**[d], and **Kersti Hermansson**[d]

[a]Department of Mechanical and Nuclear Engineering, The Pennsylvania State University, University Park, PA 16802, USA

[b]Material and Process Simulation Center, California Institute of Technology, Pasadena CA 91125, USA

[c]Department of Chemistry and Biochemistry, University of Delaware, Newark DE 19716, USA

[d]Materials Chemistry, The Ångström Laboratory Box 538, S-751 21, Uppsala University, Uppsala, Sweden

Abstract

In order to enable large-scale reactive dynamic simulations of copper oxide/water and copper ion/water interactions we have extended the ReaxFF reactive force field framework to Cu/O/H interactions. To this end, we employed a multistage force field development strategy, where the initial training set (containing metal/metal oxide/metal hydroxide condensed phase data and $[Cu(H_2O)_n]^{2+}$-cluster structures and energies) is augmented by single-point QM-energies from $[Cu(H_2O)_n]^{2+}$-clusters abstracted from a ReaxFF molecular dynamics simulation. This provides a convenient strategy to both enrich the training set and to validate the final force field. To further validate the force field description we performed molecular dynamics simulations on Cu^{2+}/water systems. We found good agreement between our results and earlier experimental and QM-based molecular dynamics work for the average Cu/water coordination, Jahn-Teller distortion and inversion in $[Cu(H_2O)_6]^{2+}$-clusters, and first- and second shell O-Cu-O angular distributions, indicating that this force field gives a satisfactory description of the Cu-cation/water interactions. We believe that this force field provides a computationally convenient method for studying the solution and surface chemistry of metal cations and metal oxides and, as such, has applications for studying protein/metal cation complexes, pH-dependent crystal growth/dissolution and surface catalysis.

1. Introduction

Copper-containing complexes play an important role in many industrial and biochemical processes. For example, copper sites in proteins activate a variety of functions including electron and oxygen transport, oxidative cleavage of biogenic amines, reduction of nitrogen

*corresponding author; acv13@psu.edu.

oxides and insertion of molecular oxygen into flavonoids. Knowledge of the local coordination environment around copper (II) in aqueous solution is essential for understanding mechanisms that regulate biological functions of these metalloproteins. Detailed information on ligand arrangement around copper (II) ion is only available in the solid state, as determined by X-ray diffraction, whereas the structural information in the aqueous phase obtained using X-ray absorption spectroscopy is more ambiguous and available only for few Cu^{2+} complexes. Although static and dynamic electronic structure calculations can, in principle, provide such information, realistic modeling of Cu complexation in aqueous solution with a highly flexible coordination sphere still remains a challenge. As such, the structure of Cu^{2+} ion in aqueous solution is not well understood despite extensive studies performed in the last two decades. Several experiments like extended x-ray absorption fine structure (EXAFS), x-ray absorption near-edge structure (XANES)1–3 as well as ab initio methods and molecular dynamics simulations4–13 have been tried to resolve this problem. For a long time, it was generally accepted that the copper(II) ion is six-fold coordinated in aqueous solution with a tetragonally distorted octahedral structure, as would be predicted from the Jahn-Teller effect for a d9 electronic configuration. This was challenged in 2001 by Pasquarello et al. who proposed a five-fold coordination based on first-principles molecular dynamics and neutron diffraction.10 Their simulation indicated frequent exchanges of square pyramidal and trigonal bipyramidal clusters with five equal Cu–O distances. One year later Persson et al. performed extensive EXAFS and large angle X-ray scattering (LAXS) experiments and again suggested that the ion was six-fold coordinated14. They modeled the copper-water cluster using several different geometrical configurations and showed that a tetragonally distorted octahedron gave the best fit to the experimental data. In 2003, a quantum-mechanical/molecular-mechanical (QM/MM) study by Schwenk et al. also indicated a six-fold coordination with Jahn-Teller distortion.12,13 However, another Car-Parrinello molecular dynamics (CPMD) simulation performed by Amira et al.4 and analysis of the XANES portion of the XAS spectra by Benfatto et al.15 and Frank et al.16 suggested that the hydrated copper (II) ion can be better represented as a five-coordinate square pyramidal structure with one elongated axial water molecule.

More recently, Chaboy et al. performed XANES and EXAFS spectroscopy of copper ion hydration17,18 and argued that “neither the classical Jahn-Teller geometry nor other six- or fivefold coordinated geometries may be proposed unambiguously as the single preferred structure in solution”.18 According to them, a dynamic view of different geometries exchanging with each other is the right description of copper ion hydration. A review of the structural parameters of Cu^{2+} aqueous complexes can be found in Reference 19.

The complicated nature of the Cu^{2+}/water system indicates that long-term (nanosecond) dynamics may be required to resolve the Cu-coordination in the aqueous phase. Such simulations are extremely time-consuming with existing QM-based methods. For this reason, attempts have been made to simulate the Jahn-Teller effect of the copper ion by incorporating special features in the standard molecular mechanical force fields.6–8 Curtiss et al. defined a reference frame that depends on the instantaneous positions of the solvent atoms and used a time-dependent rotation of the reference frame to simulate the dynamical Jahn-Teller effect of copper ion in liquid water.8 In addition to the strain energy of the

molecule, Comba et al. introduced a Jahn-Teller distortion energy based on the d-orbital splitting of the copper ion.7 Burton et al. used the d-orbital energies from the ligand field to calculate the Cellular Ligand Field Stabilization Energy (CLFSE) which has been used as an additional energy term to simulate the Jahn-Teller effect.6

In order to provide a more generalized description of the Cu/water system that properly describes the Jahn-Teller distortion and can be straightforwardly extended to describe the dynamics and reactivity of Cu-ions in bio-organic environments we have developed a ReaxFF reactive force field for Cu/O/H interactions. ReaxFF is a bond-order dependent potential that also contains a polarizable charge model20 and Coulomb interactions among all atoms (including atoms sharing a bond). ReaxFF also includes bond-order dependent 3-body (valence angles) and 4-body (dihedral) interactions. While originally developed for hydrocarbons21 we have found that the combination of covalent and ionic contributions allows formulation of ReaxFF for a wide range of materials, including covalent, metallic and ionic systems.22–26 ReaxFF is orders of magnitude faster than QM-based methods, thus enabling nanosecond-scale dynamics for large ($> 10^6$ atoms) systems.27

We have recently developed a ReaxFF potential for water and proton diffusion. This parameter set was developed against a QM-based training set containing water-dimer configurations, water-binding energies for $[H_2O]_n$ clusters (n=2–35), proton transfer barriers in OH^-/H_2O and H_3O^+/H_2O clusters as a function of O---O distance, concerted hydrogen transfer reactions in $[H_2O]_n$ clusters (n=2–6), barriers and reaction energies for water auto-dissociation, H_2, O_2 HO-OH structures and binding energies and ice(cmc) equation of state. The force field description was validated using MD-simulations on bulk water configurations as was found to reproduce the experimental density, cohesive energy, structure and diffusion constant of water; a more detailed description of this water description will be presented in a future manuscript.

Here, we describe an extension of this water potential to the Cu/O/H system. This extension involved training the Cu/O/H parameters against a QM-based database, containing structures, energies and reactions relevant to the Cu^{2+}/water system. Furthermore, to ensure the applicability of this ReaxFF potential to Cu in a wide range of environments we also included QM-data describing the Cu-metal, copper(I) and (II) oxides and copper hydroxide condensed phases in its training.

We believe that this ReaxFF Cu/O/H description provides a good basis for studying bioorganic aspects of Cu-ion chemistry, while its ability to describe Cu condensed phases opens up possibilities for studying crystal growth and corrosion-related failure of Cu-phases in aqueous environments. This paper compares the performance of the ReaxFF Cu/O/H potential against its QM-training set and also presents an initial study with this potential of the dynamics of the Cu^{2+}/water system.

2. Methods

2.1 ReaxFF: A reactive force field

ReaxFF is a bond order dependent reactive force field. The bond orders are calculated using atomic distances between every atom pairs. During an MD simulation, the evolution of the inter-atomic bond orders can modify their connectivities. Electron Equilibration Method (EEM)20 regulates the polarization and charge transfer effects in the system. The electrostatic and van der Waals interactions are calculated between every atom pairs. Reference 21,23 provide more details about the ReaxFF method.

2.2 QM-calculations for force field training and validation

2.2.1. $[Cu(H_2O)_n]^{2+}$ and $[Cu(OH)(H_2O)_n]^{+}$ clusters—The structures and energies for a series of $[Cu_x(OH)_y(H_2O)_z]^{2-y}$-clusters (Figures 4 and 5) used in the initial force field training set were obtained with the Jaguar 7.0 program package28 using the B3LYP functional. These structures were fully optimized. The application of the B3LYP method to metal ion–water systems has met with reasonable success.29–32 For open-shell Cu^{2+}-ligand systems with low coordination numbers (n=1,2) it has been reported33–35 that B3LYP binding energies are overestimated compared to CCSD(T) results. However, the B3LYP relative energies for systems with similar spin density distribution are in good agreement with those determined by highly correlated electronic structure methods.33,36 Recent calculations for $[Cu(H_2O)_n]^{2+}$ showed that B3LYP with the 6-311G++(d,p) basis set for the light atoms and the LACV3P+ basis set on Cu provides a reliable description of cluster geometries, energies and IR spectra.37,38 The same basis sets have been employed in the present study.

2.2.2. Cu, CuO, and Cu_2O crystalline phases—All calculations for the CuO and Cu_2O crystalline phases were performed using 3-dimensionally periodic systems, and the B3LYP hybrid DFT functional as implemented in the CRYSTAL06 program.39 Gaussian type basis sets as optimized by Harrison and Towler40 were used for the copper and oxygen atoms. The Brillouin zone was in all cases sampled by a 7×7×7 k-point mesh of the Monkhorst-Pack type. For CuO, spin-polarized B3LYP calculations were performed for three polymorphs having the zinc blende, the NaCl, and the monoclinic C2/*c* structure, respectively. Only the latter has been found in nature. In each case, the symmetry was lowered to allow for magnetism, and the (geometric) structure was optimized for the ferro- and anti-ferromagnetic cases. The magnetic structure that gave the lowest total energy (anti-ferromagnetic for all three polymorphs) was chosen for a subsequent calculation of the energy-volume relation. Such curves are presented in the Results and Discussion part, and the energies were used as input in the ReaxFF training set. For Cu_2O, only the (non-magnetic) cubic cuprite structure (space group $P\,n3\bar{}m$) was investigated. The structures were optimized using the CRYSTAL06 built-in geometry optimizer with default parameters. In all cases, except for monoclinic CuO, the energy-volume equation of state was created by scanning the cell axes (i.e. for the cubic lattice types). For the monoclinic phase, CRYSTAL06 built-in constant volume optimization was used to create the equation of state. The Cu-metal equations of state were obtained using the SeqQuest program.41

2.2.3 Single-point energies of $[Cu(H_2O)_5]^{2+}$ and $[Cu(H_2O)_6]^{2+}$ structures—

DFT single point energy calculations were performed on a set of $[Cu(H_2O)_5]^{2+}$ and $[Cu(H_2O)_6]^{2+}$-structures taken from MD simulations with the initial parameterization of the ReaxFF potential (see section 2.2.1). These calculations used *Gaussian 03*42 with the B3LYP functional and 6-311++g(2df,2p) basis set. A comparison between the LACV3P effective core potential (section 2.2.1) and the all-electron potential used for the $[Cu(H_2O)_5]^{2+}$ and $[Cu(H_2O)_6]^{2+}$-single point energies showed that they had very similar relative energies with excellent correlation (R^2 of 0.998), indicating that these different programs and methods provide compatible results.

2.3 MD simulations

2.3.1 Generation of $[Cu(H_2O)_5]^{2+}$ and $[Cu(H_2O)_6]^{2+}$ structures for force field training and validation—

To obtain a distribution of $[Cu(H_2O)_5]^{2+}$ and $[Cu(H_2O)_6]^{2+}$ structures for force field training and validation we performed a 133 ps long MD simulation using an initial parameterization of the ReaxFF potential. A cubic unit cell was used, 18.62 Å on each side, containing 216 water molecules and a Cu^{2+} atom. A NVT ensemble was used with a Berendsen thermostat with a damping constant of 0.1 ps. at 300 K. The density was maintained at 1.02 kg/dm^3. After 8 ps of equilibration, 45 configurations were extracted at intervals of 2.75 ps. Clusters of Cu^{2+} with its closest 5 or 6 water molecules were extracted from these configurations.

2.3.2 Simulations for radial and angular distributions and Jahn-Teller inversion—

The Cu/O radial distribution, Jahn-Teller inversion rates and O-Cu-O angular distributions were obtained from a 133 ps MD simulation with a periodic box containing 216 water molecules and a Cu^{2+} atom using a re-fitted ReaxFF potential. NVT conditions were used using the same conditions as defined in Section 2.3.1. The cubic box dimension was 18.62 Å and the density was 1.02 kg/dm^3.

3. Results and Discussion

3.1 Force field development

In order to develop a transferable ReaxFF potential for Cu/O/H interactions, with special focus on the Cu^{2+}/H_2O system, we employed the strategy employed previously by Wood et al.43:

1. Develop an initial set of parameters by training against an initial training set, consisting of the QM-data presented in Figures 2–4 ($ReaxFF^{initial}$).
2. Perform a MD simulation on a Cu^{2+}/water system using $ReaxFF^{initial}$, obtain QM-single point energies for $[Cu(H_2O)_5]^{2+}$-clusters extracted from configurations sampled from this trajectory.
3. Re-fit the ReaxFF parameters by adding these QM-single point energies to the training set. Since ReaxFF and QM use a different absolute energy scale (the zero-energy point of ReaxFF is at the fully dissociated atoms, while QM uses the separated electrons and nuclei as a zero-energy point) ReaxFF was trained against the energy difference between the QM-single point energies.

4. Validate ReaxFF^{refit} by repeating stage (2) with $[Cu(H_2O)_6]^{2+}$-clusters.

Figure 1a compares the predictions of ReaxFF^{initial} and ReaxFF^{refit} to the QM-single point energies of the $[Cu(H_2O)_5]^{2+}$-clusters, indicating that ReaxFF^{refit} provides a substantially improved fit to these QM-data. The average unsigned deviation of ReaxFF^{initial} from the QM-data is 10.8 kcal/mol, while for ReaxFF^{refit} this deviation has dropped to 4.8 kcal/mol. Compared to the cumulative water binding energy in $[Cu(H_2O)_5]^{2+}$ of about 350 kcal/mol this gives a 1.4% total average error. Furthermore, the validation against the QM-single points for the independently-created $[Cu(H_2O)_6]^{2+}$-clusters in Figure 1b demonstrates that this improvement is transferable to systems beyond the initial $[Cu(H_2O)_5]^{2+}$-clusters. The average unsigned deviation for these $Cu(H_2O)_6]^{2+}$-clusters is only somewhat bigger, 6.4 kcal/mol, than for the $[Cu(H_2O)_5]^{2+}$-clusters explicitly included in the force field optimization process. This shows that the approach of augmenting a force field training set with single-point QM-energies derived from a MD-simulation based on an approximate force field provides a fast and unbiased method for testing and validating force field parameters. All further data and discussion in this manuscript refers to the ReaxFF^{refit}-parameters.

Figures 2–6 compare the ReaxFF results to the other QM data in the training set. Figure 2 compares the ReaxFF and QM results for various Cu-metal phases, including the 12-coordinate fcc, 8-coordinate bcc, 8/6 coordinate a15, 6-coordinate simple cubic (sc) and 4-coordinate diamond phase. The volume and energies of the low-energy phases were given the most weight in the fitting, resulting in more significant discrepancies between the ReaxFF and QM results for the high-energy simple cubic and diamond phases.

Figure 3 compares the ReaxFF and QM results for copper oxide and copper hydroxide phases, indicating that ReaxFF is capable of describing the configurational landscape of the $Cu^{II}O$-phases as well as the energetics of copper oxidation and hydroxylation.

Figures 4a and 4b describe, respectively, the ReaxFF and QM water binding energies for $[Cu(H_2O)_n]^{2+}$ systems and for $[Cu(OH)(H_2O)_n]^{+}$ systems. Of specific relevance here are the $[Cu(H_2O)_n]^{2+}$ systems with H_2O bound directly to the Cu^{2+}-ions and those with H_2O associated to the water-ligands. ReaxFF correctly reproduces the QM data, favoring configurations in which one H_2O associates with the water ligands instead of directly coordinating to the Cu^{2+}-ion in the cases with more than 4 water ligands. The average unsigned deviation of ReaxFF for the $[Cu(H_2O)_n]^{2+}$ clusters (not including the irrelevant n=1 and n=2 clusters) was 1.91 kcal/mol; for the $[CuOH(H_2O)]^{+}$ clusters we obtained an average unsigned error of 3.2 kcal/mol.

To ensure that ReaxFF correctly describes the Jahn-Teller distortion around Cu^{2+}-clusters we included configurations with a fully symmetric $[Cu(H_2O)_6]^{2+}$ cluster (at various Cu-O distances) and the lower-energy distorted configuration (4 short equatorial and 2 long axial Cu-O bonds) in the ReaxFF training set. Figure 5 shows that ReaxFF indeed recognizes the distorted cluster as the global minimum. QM and ReaxFF both predict low-energy inversion barriers (0.25 and 1.08 kcal/mol, respectively) for the axial/equatorial exchange in the $[Cu(H_2O)_6]^{2+}$ cluster.

3.2 Molecular dynamics simulations on Cu^{2+}/water

3.2.1 Cu/O radial distribution and coordination—Figure 6 shows the Cu/O radial distribution function (RDF) as obtained from a molecular dynamics simulation at T=300K on a $[Cu(H_2O)_{216}]^{2+}$ system (see Methods section for a more detailed description). The RDF has a Cu-O_{eq} peak at 1.94 Å and a Cu-O_{ax} peak at 2.27 Å. These are very close to the EXAFS and LAXS peak positions of 1.95 Å for Cu-O_{eq} and 2.29 Å for Cu-O_{ax}.14 The peak representing the second hydration shell is at 4.27 Å which is close to the EXAFS and LAXS results with a mean distance of 4.17 Å.14 Thus, this copper potential provides a good model of the Jahn-Teller effect in copper hydrate as the water molecules have distinct preferences for taking either the axial or the equatorial positions rather than lying between them. This is comparable to the other theoretical models based on sophisticated methodologies like QM/MM12,13 or CPMD4 that could provide a satisfactory description of the structural properties of the hydrated copper (II) ion. A comparison of the geometrical features of copper hydration with a few references from the literature is shown in Table 1 (a more comprehensive list can be found in Reference 4). Our results fall well within the ranges of both experimental and theoretical observations. Integration of the RDF to a distance of 2.14 Å, where the RDF has a trough between the two peaks, shows a coordination number of 3.91 (Figure 6). This roughly corresponds to the 4 equatorial water molecules in a plane with the copper ion. The integral reaches a coordination number of six at 2.44 Å and retains this value until 3.49 Å, indicating negligible water exchange between the first and the second hydration shells during the 125 ps simulation time.

Clusters of copper with the nearest six water molecules were visualized directly to examine their geometries. We found in most cases that the farthest two water molecules from the copper ion were axially opposite to each other, forming a tetragonally distorted octahedral geometry. The few exceptions, where they made an angle of about 90° with the copper ion, probably reflect configurations capturing the dynamic switching of the elongation axis (Jahn-Teller inversion).

3.2.2 Jahn-Teller inversion—A special feature of the dynamics of Cu^{2+}-water interaction is the Jahn-Teller inversion. Experimental studies like electron spin resonance44 (ESR) and ^{17}O NMR45 as well as computational methodologies like QM/MM12,13 have shown that the axis of distortion of the Cu^{2+}-water cluster randomly reorients at a much faster rate than the exchange rate of water molecules between the first solvation shell and the bulk. Powell et al.45 used ^{17}O NMR to estimate τ_i, the mean lifetime between two inversions to be 5.1 ps. Later, Schwenk et al. suggested that τ_i should be less than 200 fs based on QM/MM studies.12,13 They postulated that the Jahn-Teller inversion is an extremely fast phenomenon taking place on a sub-picosecond time scale.

Figure 7 shows the time evolution of the distances between two oxygen atoms in the first solvation shell, on opposite sides of the copper ion, during the last 75 ps of our simulation. Several distinct intervals can be seen where one of the O-O distances is around 4.4 Å while the other two are around 3.9 Å, reflecting the Jahn-Teller distortion. The calculation of the inversion rate was not straightforward, because it was not clear at certain points if the relative changes in the three distances were significant enough to be counted as a true

inversion. There were several approaches to inversion of the distortion axis but the original orientation was recovered within a fraction of a picosecond. We could detect 13 certain and 4 subtle inversions during the 75 ps simulation giving a value of τ_i of approximately 5 ps closely matching the experimental value of 5.1 ± 0.6 ps obtained by Powell et al.45 This level of agreement is remarkable, especially given the difference between the ReaxFF and QM-barriers for Jahn-Teller inversion in Figure 5. Given, however, that this ReaxFF/QM difference is well within the error-margin of the QM-method employed here, it may be that ReaxFF inadvertently obtained an inversion barrier that is more accurate than the QM-result, thus explaining the agreement with experiment.

Figure 7 also shows a few time intervals where all the three distances are comparable to each other. A visualization of the clusters confirmed that although the two elongated Cu^{2+}-water distances are mostly on opposite sides of the ion, in a few configurations they make a 90° angle. In a few other configurations, more than two Cu^{2+}-water pairs were elongated. These irregularities contributed to the randomness observed in a few places in Figure 7. These have also been reported by Schwenk et al.12,13 and illustrate fluctuations in the Jahn-Teller distortion.

3.2.3 ∠(O-Cu-O) Angular Distribution—The structures of the Cu^{2+}-water solvation shell have also been analyzed by the ∠(O-Cu-O) angular distribution function. The first hydration shell with 6 water molecules shows two distinct peaks at 90° and 176° (Figure 8a) as expected for an octahedral geometry. These values match closely with both QM/MM12,13 and CPMD4 results (Table 1). Water molecules in the second hydration shell (W2) are also structured because they form hydrogen bonds with water molecules in the first hydration shell (W1). A direct visualization of these structures indicates that W1 molecules make hydrogen bonds with W2 molecules and they are not collinear with Cu^{2+}. Figure 8b shows the ∠(O-Cu-O) angular distribution for the 14 closest water molecules. The peaks at 90° and 176° are primarily due to waters in the first hydration shell, while the peaks near 30°, 60°, 120° and 150° correspond to waters in the second solvation shell (Figures 8a and 8b).

3.2.4 Cu^{2+} coordination—To confirm our postulate that the force field favors a six-fold coordination for the Cu^{2+}-ion in solution, we performed a set of molecular dynamics simulations with different initial configurations. From the end point of a simulation that included a six-fold coordinated Cu^{2+}-ion, we removed two axially opposite water molecules in the first hydration shell to produce a square planer geometry and started a new simulation from that configuration. Five-fold square pyramidal coordination was recovered within 11 ps and six-fold octahedral coordination was reached in the succeeding 26 ps. It remained six-fold coordinated for the rest of the simulation. We performed the same procedure starting with a five-fold square pyramidal configuration. Six-fold octahedral coordination was recovered in 8 ps and the ion remained six-fold coordinated for the rest of the simulation. This simulation procedure was repeated a number of times from independent six-fold coordinate Cu^{2+}-ions; in all cases we found the 4-fold to 5-fold transition to be very fast (always within 15 ps.), but the 5- to 6-fold transition time had a considerably larger

variation; in one particular case the 5-fold complex survived for the entire duration of the simulation (125 ps.).

Considering the lifetime of the five fold coordination in these simulations, its existence cannot be ignored. It is reasonable to think that copper might form a five-fold coordination for short time intervals during a long simulation dominated by six-fold coordination.

4. Conclusions

In order to enable large-scale reactive dynamics simulations on copper oxide/water and copper ion/water interactions we have extended the ReaxFF reactive force field framework to Cu/O/H interactions. To this end, we employed a multistage force-field development strategy, where the initial training set (containing metal/metal oxide/metal hydroxide condensed phases data and $[Cu(H_2O)_n]^{2+}$-cluster structures and energies) is augmented by single-point QM-energies for $[Cu(H_2O)_n]^{2+}$-clusters sampled from a ReaxFF molecular dynamics simulation. This provides a convenient strategy to both enrich the training set and to validate the final force field. To further validate the force field description we performed molecular dynamics simulations on Cu^{2+}/water systems. We found good agreement between our results and earlier experimental and QM-based molecular dynamics work for average Cu/water coordination, Jahn-Teller distortion and inversion, and first- and second shell O-Cu-O angular distributions, indicating that this force field gives an accurate description of the Cu-cation/water interactions. We believe that this force field provides a computationally convenient method for studying the solution and surface chemistry of metal cations and metal oxides and, as such, has applications for studying protein/metal cation complexes, pH-dependent crystal growth/dissolution and surface catalysis.

Supplementary Material

Refer to Web version on PubMed Central for supplementary material.

Acknowledgments

The Caltech portion of the work was carried out at the Materials and Process Simulation Center of the Division of Chemistry and Chemical Engineering. Funding for the Caltech work was provided by the National Science Foundation (CBET NIRT 0948485, CTS-0506951), EPA STAR (RD 832525) and ORNL (6400007192). The work in Uppsala University was supported by the Swedish Research Council (VR). Work at the University of Delaware was partially supported by a grant (P42 ES010344-06A2 Sub Award# 09-1535) from the National Institute of Environmental Health Sciences, one of the National Institutes of Health. ACTvD acknowledges funding from KISK startup grant #C000032472.

References

1. Nomura M, Yamaguchi T. J Phys Chem-Us. 1988; 92:6157.
2. Beagley B, Eriksson A, Lindgren J, Persson I, Pettersson LGM, Sandstrom M, Wahlgren U, White EW. J Phys-Condens Mat. 1989; 1:2395.
3. Garcia J, Benfatto M, Natoli CR, Bianconi A, Fontaine A, Tolentino H. Chem Phys. 1989; 132:295.
4. Amira S, Spangberg D, Hermansson K. Phys Chem Chem Phys. 2005; 7:2874. [PubMed: 16189606]
5. Burda JV, Pavelka M, Simanek M. J Mol Struc-Theochem. 2004; 683:183.

6. Burton VJ, Deeth RJ, Kemp CM, Gilbert PJ. Journal of American Chemical Society. 1995; 117:8407.
7. Comba P, Zimmer M. Inorg Chem. 1994; 33:5368.
8. Curtiss L, Halley JW, Wang XR. Phys Rev Lett. 1992; 69:2435. [PubMed: 10046484]
9. Marini GW, Liedl KR, Rode BM. Journal of Physical Chemistry A. 1999; 103:11387.
10. Pasquarello A, Petri I, Salmon PS, Parisel O, Car R, Toth E, Powell DH, Fischer HE, Helm L, Merbach AE. Science. 2001; 291:856. [PubMed: 11157161]
11. Pavelka M, Simanek M, Sponer J, Burda JV. Journal of Physical Chemistry A. 2006; 110:4795.
12. Schwenk CF, Schwenk CF, Rode BM. Chemphyschem. 2003; 4:931. [PubMed: 14562438]
13. Schwenk CF, Rode BM. Journal of Chemical Physics. 2003; 119:9523.
14. Persson I, Persson P, Sandstrom M, Ullstrom AS. J Chem Soc Dalton. 2002:1256.
15. Benfatto M, D'Angelo P, Della Longa S, Pavel NV. Phys Rev B. 2002; 65:174205.
16. Frank P, Benfatto M, Szilagyi RK, D'Angelo P, Della Longa S, Hodgson KO. Inorg Chem. 2005; 44:1922. [PubMed: 15762718]
17. Chaboy J, Munoz-Paez A, Carrera F, Merkling P, Marcos ES. Phys Rev B. 2005; 71
18. Chaboy J, Munoz-Paez A, Merkling PJ, Marcos ES. Journal of Chemical Physics. 2006; 124
19. Smirnov PR, Trostin VN. Russ J Gen Chem+. 2009; 79:1591.
20. Mortier WJ, Ghosh SK, Shankar S. J Am Chem Soc. 1986; 108:4315.
21. van Duin ACT, Dasgupta S, Lorant F, Goddard WA. Journal of Physical Chemistry A. 2001; 105:9396.
22. Chenoweth K, Cheung S, van Duin ACT, Goddard WA, Kober EM. J Am Chem Soc. 2005; 127:7192. [PubMed: 15884961]
23. van Duin ACT, Strachan A, Stewman S, Zhang QS, Xu X, Goddard WA. Journal of Physical Chemistry A. 2003; 107:3803.
24. Buehler MJ, van Duin ACT, Goddard WA. Phys Rev Lett. 2006; 96
25. Cheung S, Deng WQ, van Duin ACT, Goddard WA. Journal of Physical Chemistry A. 2005; 109:851.
26. Raymand D, van Duin ACT, Baudin M, Hermansson K. Surf Sci. 2008; 602:1020.
27. Nakano A, Kalia RK, Nomura K, Sharma A, Vashishta P, Shimojo F, van Duin ACT, Goddard WA III, Biswas R, Srivastava D. Comp Mater Sci. 2007; 38:642.
28. Jaguar, v. New York, NY: Schrödinger, LLC; 2007.
29. Carl DR, Moision RM, Armentrout PB. Int J Mass Spectrom. 2007; 265:308.
30. Marino T, Toscano M, Russo N, Grand A. J Phys Chem B. 2006; 110:24666. [PubMed: 17134229]
31. Peschke M, Blades AT, Kebarle P. J Am Chem Soc. 2000; 122:10440.
32. Tunell I, Lim C. Inorg Chem. 2006; 45:4811. [PubMed: 16749846]
33. Bertran J, Rodriguez-Santiago L, Sodupe M. J Phys Chem B. 1999; 103:2310.
34. Georgieva I, Trendafilova N, Rodriguez-Santiago L, Sodupe M. Journal of Physical Chemistry A. 2005; 109:5668.
35. Poater J, Sola M, Rimola A, Rodriguez-Santiago L, Sodupe M. Journal of Physical Chemistry A. 2004; 108:6072.
36. Rimola A, Rodriguez-Santiago L, Ugliengo P, Sodupe M. J Phys Chem B. 2007; 111:5740. [PubMed: 17469869]
37. Bryantsev VS, Diallo MS, van Duin ACT, Goddard WA. Journal of Physical Chemistry A. 2008; 112:9104.
38. OBrien JT, Williams ER. Journal of Physical Chemistry A. 2008; 112:5893.
39. http://www.crystal.unito.it/
40. http://www.tcm.phy.cam.ac.uk/~mdt26/basis_sets/Cu_basis.txt
41. Schultz, PA. SeqQuest. Alburquerque, NM: Sandia National Labs; http://dft.sandia.gov/Quest/
42. Frisch, MJ., et al. G., Revision C. 02. Wallingford CT: Gaussian, Inc.; 2004.
43. Wood RH, Yezdimer EM, Sakane S, Barriocanal JA, Doren DJ. Journal of Chemical Physics. 1999; 110:1329.

44. Poupko R, Luz Z. Journal of Chemical Physics. 1972; 57:3311.
45. Powell DH, Helm L, Merbach AE. Journal of Chemical Physics. 1991; 95:9258.

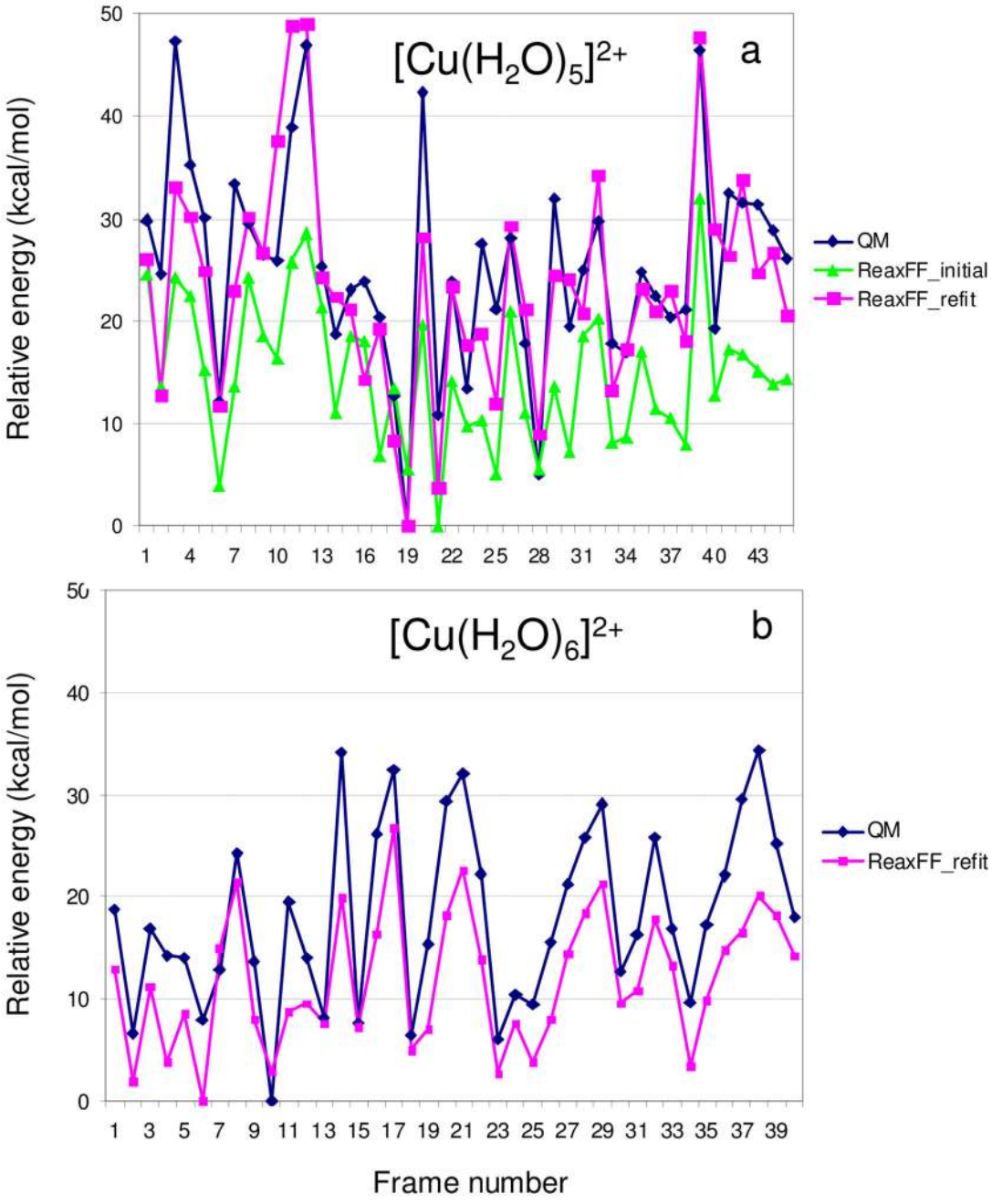

Figure 1.

(a) Initial results (ReaxFF_initial) and refitted results (ReaxFF_refit) for the comparison between QM-single point energies for $[Cu(H_2O)_5]^{2+}$-clusters taken from a MD-simulation using ReaxFF_initial. Energies are plotted relative to the most stable cluster (b) comparison between results for the refitted ReaxFF parameters to QM-single point energies for $[Cu(H_2O)_6]^{2+}$-clusters taken from a MD-simulation using ReaxFF_refit.

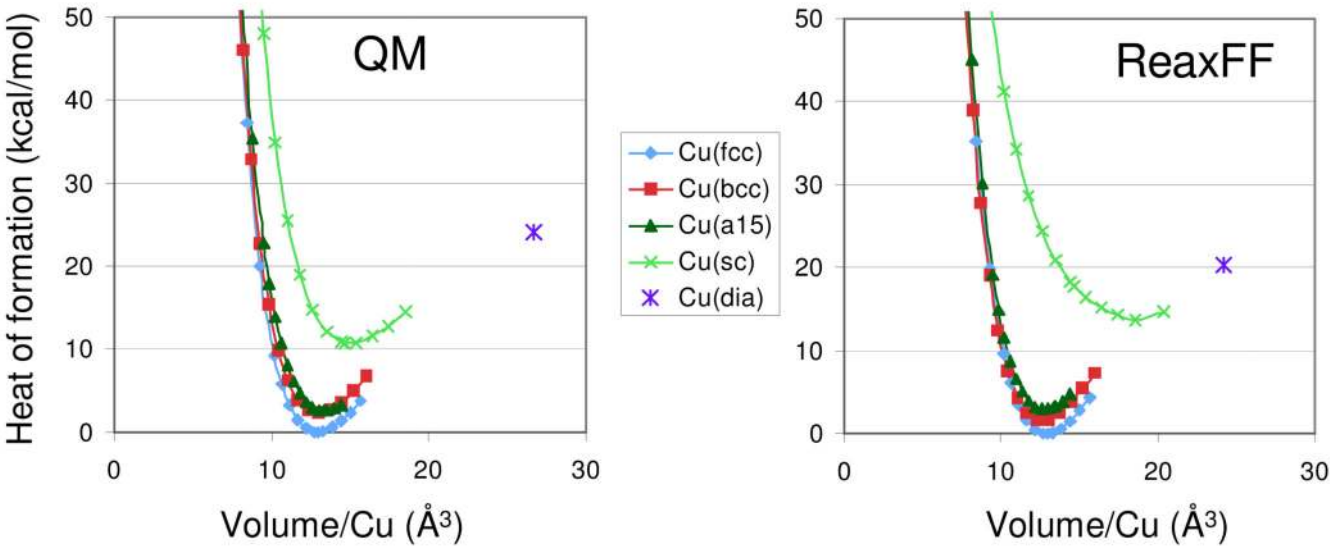

Figure 2.

QM- and ReaxFF equations of state for Cu-metal polymorphs. ReaxFF obtains a cohesive energy of 81.2 kcal/mol for the Cu-fcc phase, compared to and experimental value of 80.7 kcal/mol.

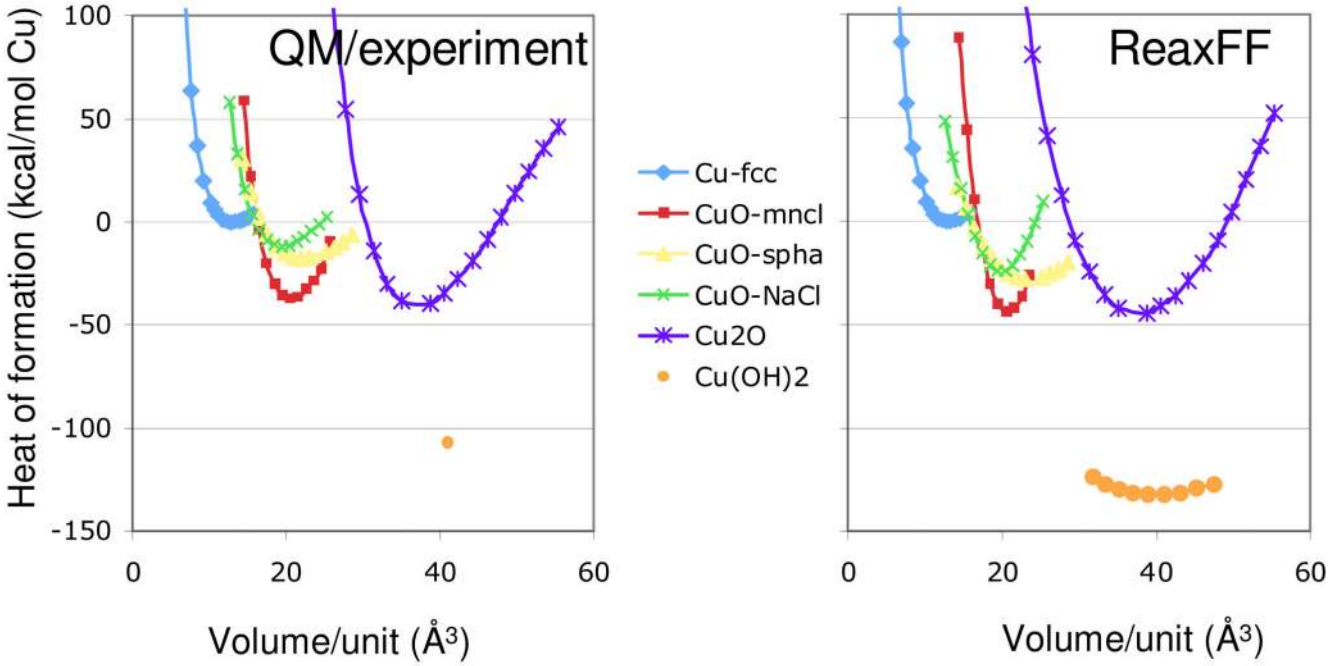

Figure 3.

QM/experiment and ReaxFF results for heats of formation and equations of state for Cu-metal, CuO, Cu_2O and $Cu(OH)_2$ crystalline phases. Heats of formation for the CuO(mncl), Cu_2O (cuprite) and $Cu(OH)_2$-phases were taken from experiment; the QM-data was used expand these experimental heats of formation to equations of state.

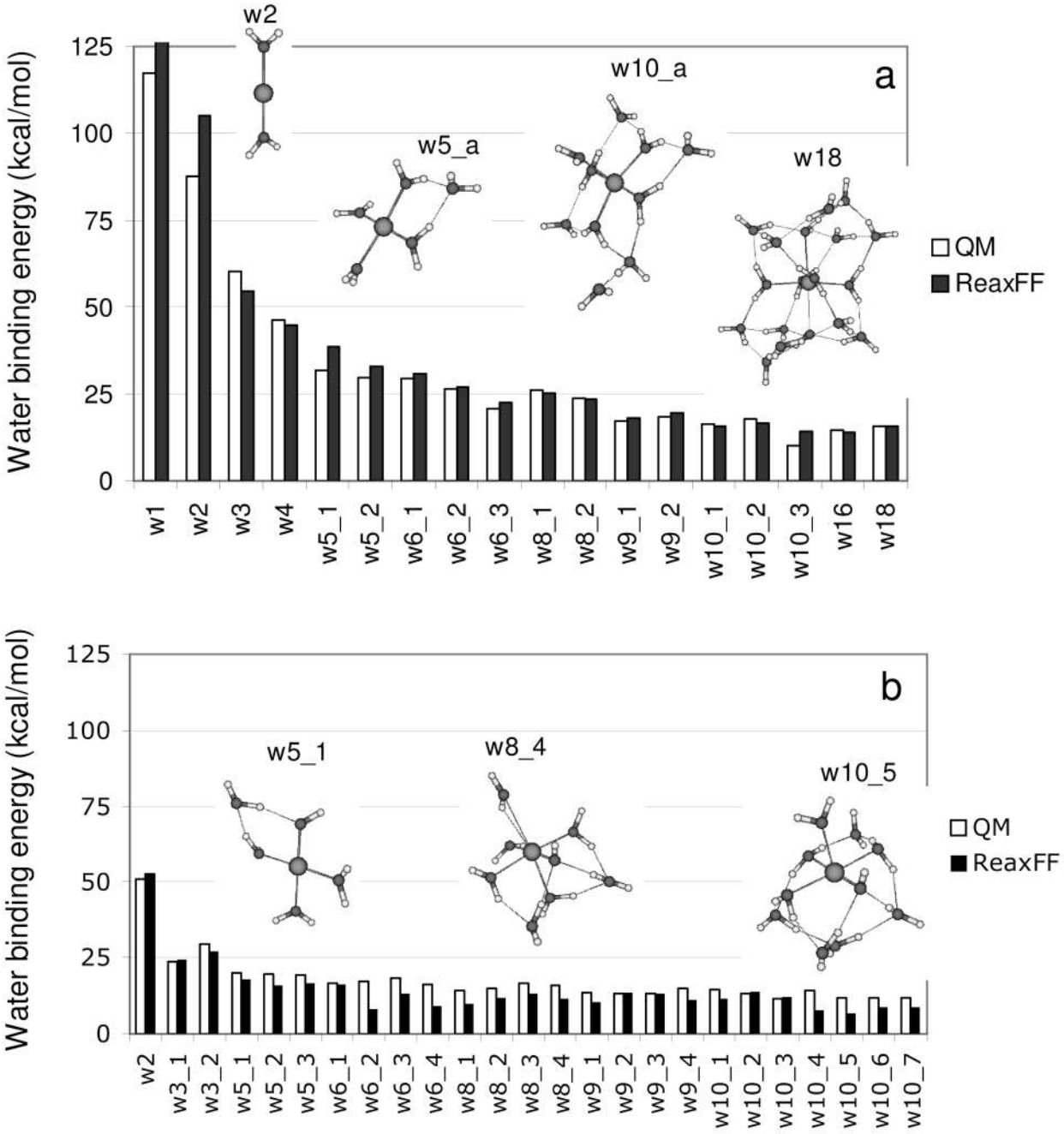

Figure 4.

QM- and ReaxFF water binding energies to $[Cu(H_2O)_n]^{2+}$ (a) and $[CuOH(H_2O)_n]^{+}$ clusters (b). In the cluster notation w(x_y) x describes the number of water molecules (or water molecules + OH) around the copper ion, while y describes the configuration number (e.g. we included four configurations, w8_1 to w8_4, for the $[CuOH(H_2O)_8]^{+}$-cluster). QM data were taken from ref. 37. Binding energies were defined as $E([Cu(OH)_y(H_2O)_x]) + E(H_2O) - E([Cu(OH)_y(H_2O)_x])$.

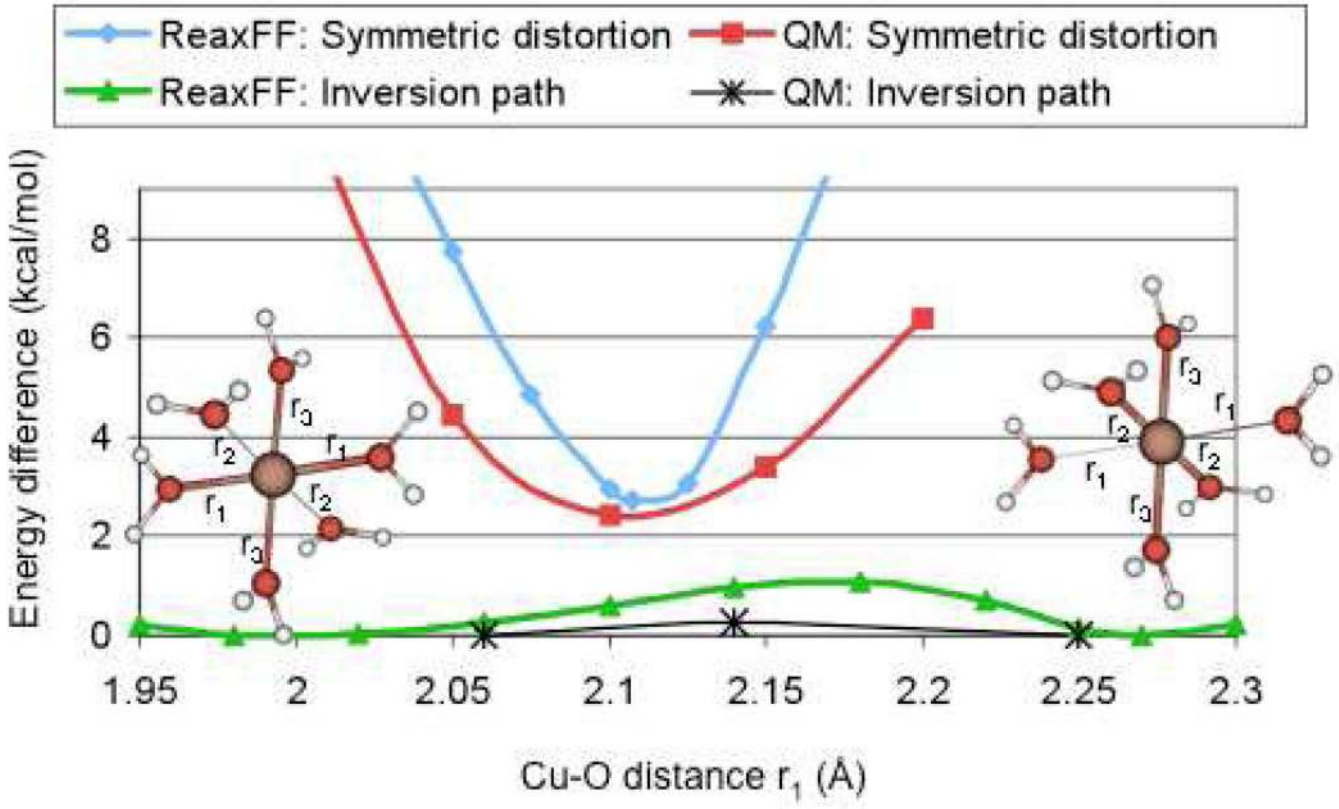

Figure 5.

QM- and ReaxFF results for the bond distortion (bond stretching and compression) of a symmetric $[Cu(H_2O)_6]^{2+}$-cluster ($r_1=r_2=r_3$) and for the inversion path of a Jahn-Teller distorted $[Cu(H_2O)_6]^{2+}$-cluster. As indicated in the figure, both QM and ReaxFF predict the distorted cluster to be about 2.5 kcal/mol more stable than the symmetric cluster and the transition state for the Jahn-Taller inversion is more stable than the symmetric cluster.

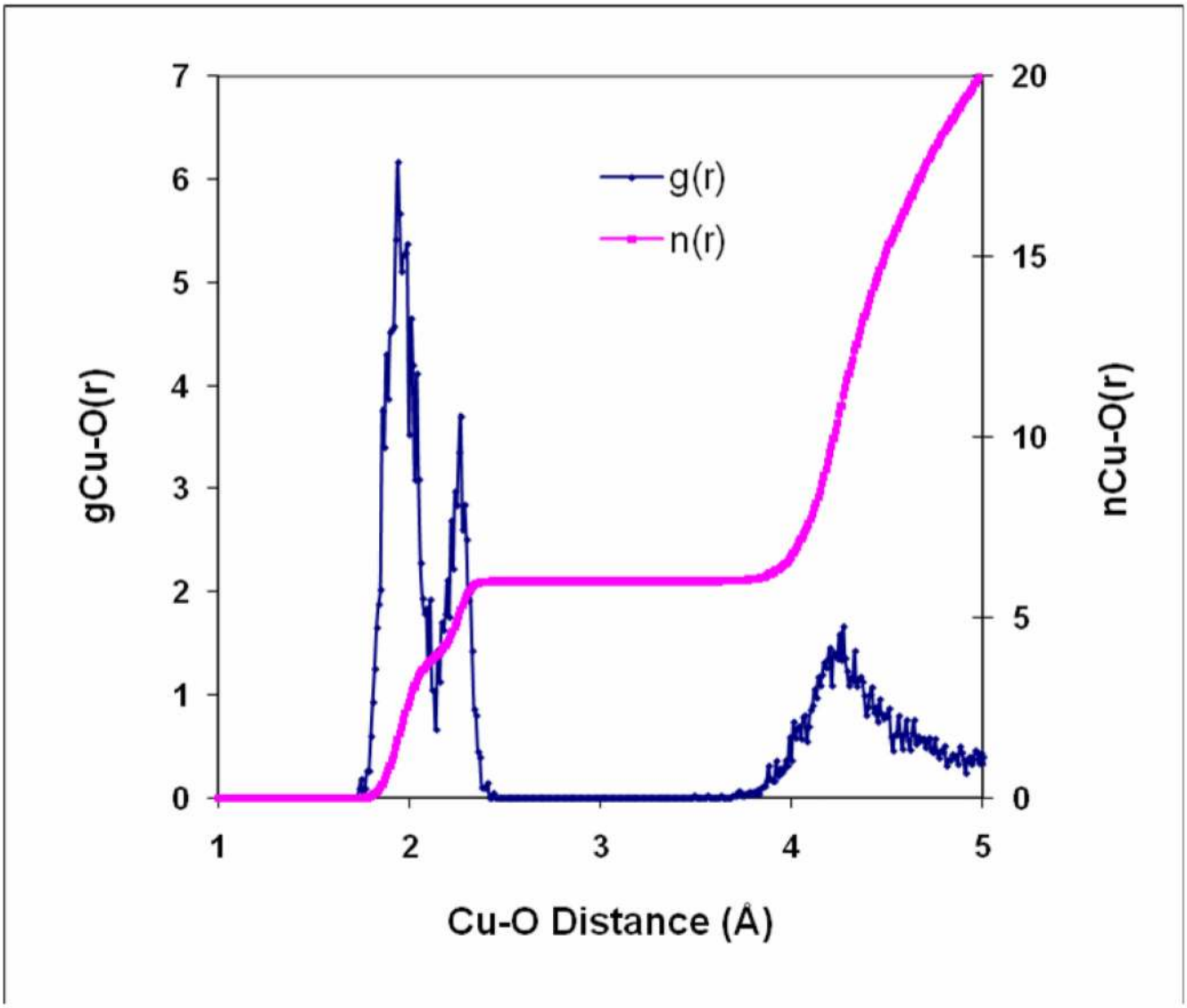

Figure 6.

Cu-O radial distribution function and integral as obtained from a ReaxFF molecular dynamics simulation on a $[Cu(H_2O)_{216}]^{2+}$ system at T=300K

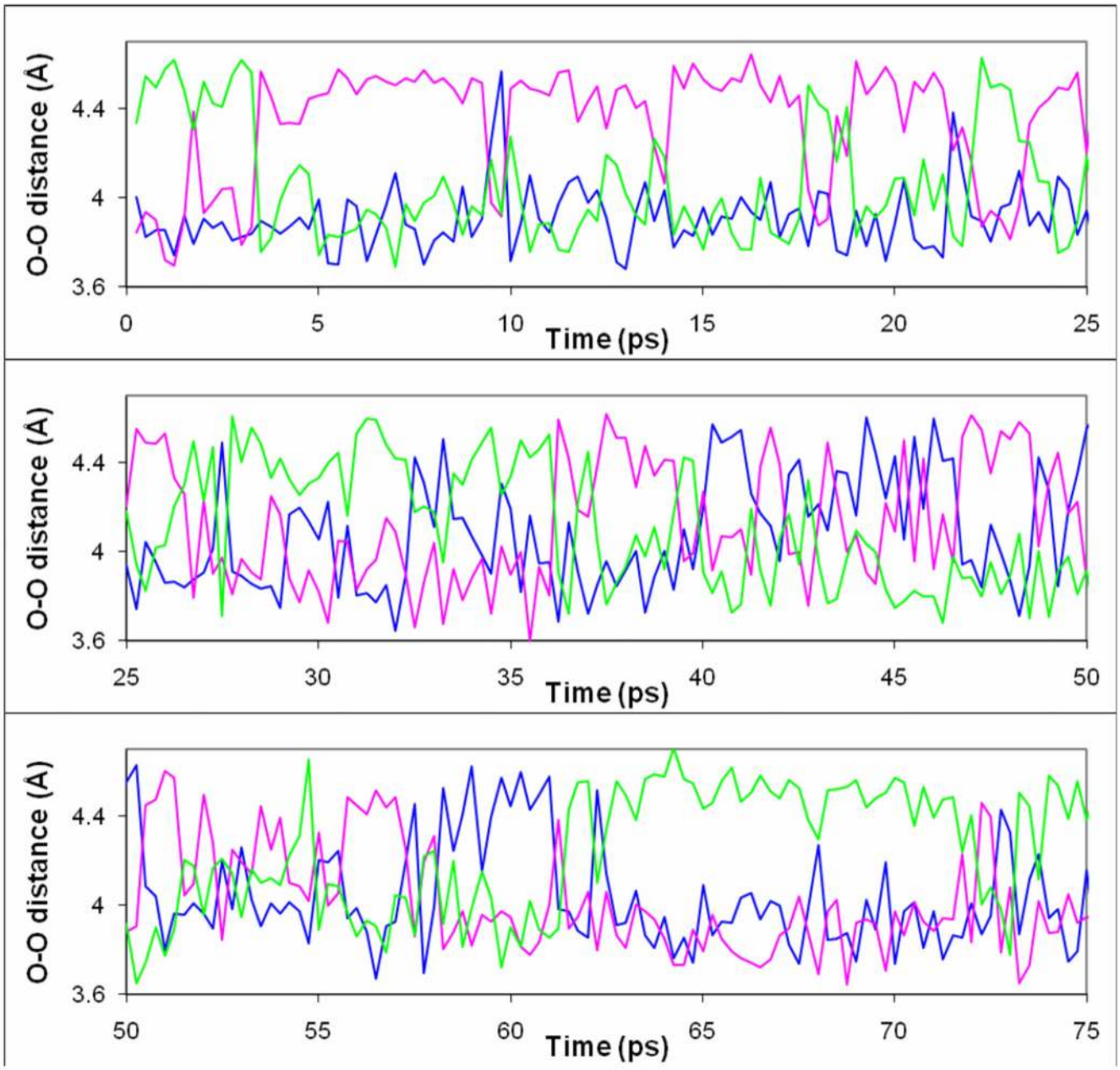

Figure 7.

Time evolution of O—O distances around the $[Cu(H_2O)_6]^{2+}$ complex during a 75 ps ReaxFF molecular dynamics simulation on a $[Cu(H_2O)_{216}]^{2+}$ system at T=300K

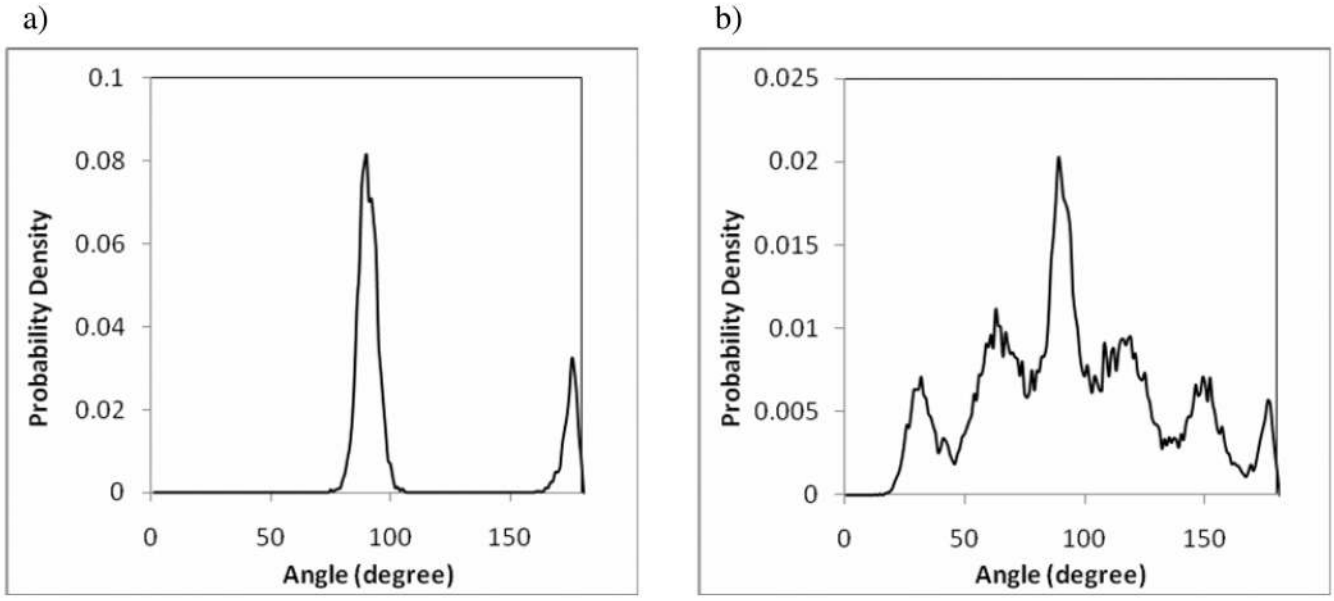

Figure 8.

∠(O-Cu-O) angular distribution observed during a ReaxFF molecular dynamics simulation of aqueous Cu^{2+}, showing a) only the six water molecules in the first hydration shell and b) the nearest 14 water molecules.

Table 1

Cu-O distances for equatorial (Cu-O_{eq}), axial (Cu-O_{ax}), and second shell waters (Cu-$O_{2ndshell}$), the 1st and 2nd shell coordination numbers (CN) and the ∠(O-Cu-O) angular distribution peaks from the ReaxFF MD-simulations (this work) and as observed in other theoretical and experimental work. The 2nd shell coordination number was obtained by integrating the ReaxFF rdf (Figure 6) between r(Cu-O)=3 to r(Cu-O)=4.8. The second solvation shell peak does not completely return to zero, making the CN 2nd assignment somewhat arbitrary.

Method	Cu-O_{eq} (Å)	Cu-O_{ax} (Å)	CN 1st	Cu-$O_{2nd\ shell}$	CN 2nd	∠(O-Cu-O)
This work	1.94	2.27	6	4.27	12.5	90, 176
EXAFS/LAXS14	1.95	2.29	6	4.17	8	
B3LYP QM/MM12,13	2.02	2.29	6	4.13	11.9	89, 173
CPMD10	1.96	1.96	5			
CPMD4	2.00	2.45	5	4.03	8	90, 180